

Neurophysiological differences between patients clinically at high risk for schizophrenia and neurotypical controls – first steps in development of a biomarker

RESEARCH ARTICLE

Open Access



Neurophysiological differences between patients clinically at high risk for schizophrenia and neurotypical controls – first steps in development of a biomarker

Frank H. Duffy^{1*}, Eugene D'Angelo², Alexander Rotenberg¹ and Joseph Gonzalez-Heydrich²

Abstract

Background: Schizophrenia is a severe, disabling and prevalent mental disorder without cure and with a variable, incomplete pharmacotherapeutic response. Prior to onset in adolescence or young adulthood a prodromal period of abnormal symptoms lasting weeks to years has been identified and operationalized as clinically high risk (CHR) for schizophrenia. However, only a minority of subjects prospectively identified with CHR convert to schizophrenia, thereby limiting enthusiasm for early intervention(s). This study utilized objective resting electroencephalogram (EEG) quantification to determine whether CHR constitutes a cohesive entity and an evoked potential to assess CHR cortical auditory processing.

Methods: This study constitutes an EEG-based quantitative neurophysiological comparison between two unmedicated subject groups: 35 neurotypical controls (CON) and 22 CHR patients. After artifact management, principal component analysis (PCA) identified EEG spectral and spectral coherence factors described by associated loading patterns. Discriminant function analysis (DFA) determined factors' discrimination success between subjects in the CON and CHR groups. Loading patterns on DFA-selected factors described CHR-specific spectral and coherence differences when compared to controls. The frequency modulated auditory evoked response (FMAER) explored functional CON–CHR differences within the superior temporal gyri.

Results: Variable reduction by PCA identified 40 coherence-based factors explaining 77.8 % of the total variance and 40 spectral factors explaining 95.9 % of the variance. DFA demonstrated significant CON–CHR group difference ($P < 0.00001$) and successful jackknifed subject classification (CON, 85.7 %; CHR, 86.4 % correct). The population distribution plotted along the canonical discriminant variable was clearly bimodal. Coherence factors delineated loading patterns of altered connectivity primarily involving the bilateral posterior temporal electrodes. However, FMAER analysis showed no CON–CHR group differences.

Conclusions: CHR subjects form a cohesive group, significantly separable from CON subjects by EEG-derived indices. Symptoms of CHR may relate to altered connectivity with the posterior temporal regions but not to primary auditory processing abnormalities within these regions.

Keywords: Biomarker, Clinical high risk, Discriminant function analysis, Electroencephalogram spectral coherence, Frequency modulated auditory evoked response, Principal component analysis, Prodrome, Schizophrenia

* Correspondence: fhd@sover.net

¹Department of Neurology, Boston Children's Hospital and Harvard Medical School, 300 Longwood Ave, Boston, Massachusetts 02115, USA
Full list of author information is available at the end of the article

Background

Schizophrenia is a chronic, severe, and disabling mental disorder characterized by deficits in thought processes, perceptions, and emotional responsiveness. Furthermore, it is associated with symptoms including cognitive disorganization, hallucinations, and paranoia. The prevalence per year in the USA is 1.1 % of the adult population (www.nimh.nih.gov/health/topics/schizophrenia).

The yearly incidence for psychotic disorders has been reported recently in Australia as 28 per 100,000 population, with rates peaking in adolescence and young adulthood [1]. However, a longitudinal register-based case finding approach, as opposed to a first-contact sampling approach, clarified that the incidence of schizophrenia is likely many times higher than commonly reported, reaching as high as 69 per 100,000 patients per year in the USA [2].

Medications have failed to 'cure' schizophrenia and response to pharmacologic intervention is reported to be quite variable [3], which may relate in part to poor medication compliance [4] and may also have biological underpinnings. For example, 30 % of patients with inadequate medication response had a group-specific magnetic resonance imaging (MRI) pattern of marked frontal atrophy [5]. Many publications suggest that, although schizophrenia cannot be medically 'cured', various support strategies including social, psychological, and environmental – as well as pharmacologic – may prove substantially ameliorative and suggest that the course of schizophrenia be considered 'uneven' rather than 'chronic' [6–8].

Schizophrenia has been increasingly viewed from a developmental perspective. Full psychosis appears to represent a later aspect of the disorder. This raises the possibility that medical and/or pharmacologic interventions provided early might be of greater help to patients in the long term. As reviewed by Larson et al. [3], prior to onset of diagnosed schizophrenia in adolescence or young adulthood, and prior to persistent psychosis, there may be a 'prodromal' or clinical high risk (CHR) period, lasting from several weeks to several years, during which aberrant behaviors are evident.

Although the notion of neurodevelopmental influences upon schizophrenia originally arose from postulated changes in fetal brain development [9], more recent thinking also suggests a contribution from abnormalities during adolescent brain development. Larson et al. [3] summarized that "...persons later diagnosed with schizophrenia ...[may show]... early intellectual and neuromotor disabilities" [10–14]. By the first episode of psychosis, those affected on average exhibit slightly larger cerebral ventricles and slightly less central gray matter than healthy controls [15]. These findings support the notion that at least part of the disease process appears to be developmental.

CHR for schizophrenia is typically observed in adolescents and young adults who manifest disturbances in stress

tolerance, perception, cognitive function, language, motor function, energy, and initiative [16]. Although paranoia and hallucinations may be intermittently reported during the CHR phase, they are recognized by the patient as 'not real'. The CHR phase 'ends' and the diagnosis of psychosis reached when the episodes of paranoia and hallucinations become much more frequent and reality testing wanes. Approximately 20–40 % of subjects with CHR go on to develop psychosis and full-onset schizophrenia [17–22]. Approximately 60–80 % of the subjects with CHR who proceed from prodrome to psychosis can be variably predicted based upon severity of pre-psychotic symptomatology [3].

The ultimate outcome of those patients with CHR symptoms who do not 'convert' is poorly established; most continue to exhibit an array of cognitive and behavioral issues. Some are later diagnosed with schizotypal disorder, in the absence of psychosis. Some investigators have questioned whether subjects with CHR symptoms, who do not convert to schizophrenia, should constitute a separate syndrome [23]. Treatment of CHR with atypical antipsychotics, antidepressants, cognitive therapy, or fish oils may result in behavioral improvement; however, initial favorable response to these treatments may not result in long term benefits following treatment cessation [3, 24–29]. A more recent study suggests that fish oils may be of preventative value [30]. The rate of non-conversion, the difficulties prospectively identifying the converters, and the risks of available treatments and stigmatization has made preventive treatment complex.

MRI studies of CHR have variably documented findings of reduction in frontal and temporal grey matter volumes with suggestion that such imaging data could help determine the risk of psychotic manifestations [15, 31–33]. However, an important study by Owens et al. [34] served to diminish these expectations. These authors contrasted MRI-acquired measures of prefrontal cortex grey matter volume reductions and of neuropsychological measures of mental executive function in close relatives of patients with schizophrenia. MRI prefrontal abnormalities were not shown to be familial whereas the neuropsychological findings were familial. The authors concluded "...that the well-recognized prefrontal volume reductions ...[in schizophrenia]... are not related to the same familial influences that increase schizophrenia liability and, instead, may be attributable to illness related biological changes or indeed confounded by illness trajectory, chronicity, medication or substance abuse, or in fact a combination of some or all..." [34].

As has been summarized [35], it remains generally agreed that electroencephalogram (EEG) evaluation by traditional, unaided visual inspection bears scant clinical or scientific fruit for the study of psychiatric patients – aside from its value in excluding epilepsy. This contrasts with an

abundance of published evidence that numerical quantification of EEG by spectral and related spectral coherence analyses have demonstrated “...high proportions of abnormal findings... with good concordance and high specificity... across numerous studies... [in psychiatric disorders]” [36]. Spectral analysis refers to the quantitative analysis of EEG frequency across spectral bands (e.g. delta, theta, alpha, beta, and gamma) typically by Fast Fourier Transform (FFT) [37, 38]. Spectral coherence refers to the assessment, on a frequency by frequency basis, of the phase difference between the signals from two EEG channels as compared over time. As Duffy and Als stated [35], “Spectral coherence is a measure of synchronization between two... [EEG]... signals based mainly on phase consistency; that is, two signals may have different phases... [differing relative temporal shifts]... but high coherence occurs when this phase difference tends to remain constant over time” [39]. High coherence values are taken as a measure of strong connectivity or coupling between the brain regions that produce the compared EEG signals [37].

Early studies of EEG spectral background in schizophrenia demonstrated excessive frontal delta slowing [40, 41]; however, a later study demonstrated that a major component of the frontal slowing could be attributed to residual frontal eye blink delta band artifact that may survive visually-based attempts at blink removal. Eye blinking has been documented to be more prominent in subjects with schizophrenia [42]. Furthermore, increased spontaneous eye blink frequency has also been well-documented in schizophrenia [43].

Many studies have subsequently evaluated EEG spectral coherence in schizophrenia [44–50]; overall results suggested an increase of both inter- and intra-hemispheric coherence. Indeed, Mann et al. [46] concluded, on the basis of their group data analyses, that “Increased coherence might be assumed to be a vulnerability marker for schizophrenia reflecting maldevelopment of the brain before onset of the disorder.” However, during hallucinations, working memory tests and photic stimulation, others have found that coherence may be relatively reduced in schizophrenia [44, 48, 50].

Recently, there has been a focus on the gamma EEG spectral band in schizophrenia [51–60]. This interest arises as cortical gamma oscillation appears to be involved in both local and large-scale neuronal synchronization underlying a number of perceptual and higher order cognitive functions of the sort often found to be abnormal in schizophrenia [51]. Unfortunately, the background EEG gamma spectral band and the spectral band of ambient waking scalp muscle activity, as evidenced in scalp EEG recordings, almost exactly overlap [61]. It has further been observed that ‘thinking’ activates scalp muscle artifact [62]. In addition, the induced gamma-band EEG response (iGBR) recorded on the scalp in response to external

stimuli, such as in evoked potential studies, is widely assumed to reflect synchronous neural oscillation associated with object representation, attention, memory, and consciousness. However, it has been suggested that the visual iGBR recorded within scalp EEG may actually reflect properties of visually induced miniature saccade dynamics rather than neuronal oscillations [63, 64], although this has been contested [65]. More recently, it has been reported that auditory iGBR recorded on the scalp may also be affected by saccadic muscle activity [66]. Hence, until signal processing reaches the point where scalp muscle-generated gamma artifact and true scalp recorded cortical gamma activity contributions can be differentiated cleanly and reliably within traditional EEG recordings, scalp frequencies above 30 Hz (gamma) must be considered to be unreliable for the purposes of spectral and coherence analyses, since gamma spectral data appear to be seriously contaminated by background and/or induced muscle activity. Clinical differences of scalp EEG activity between groups in a comparison study of schizophrenic patients and neurotypical control (CON) subjects could result in spurious, albeit statistically significant, high frequency gamma band spectral and/or coherence between groups. To quote Whitham et al. [62] “...severe restrictions exist on utilizing scalp recordings for high frequency EEG”.

The intent of the current study was to search for consistent scalp EEG differences (by quantitative spectral and spectral coherence analyses) between patients with CHR for schizophrenia and CON subjects. The goal was to determine (1) whether ambient, waking state EEG recordings provide data which allow reliable group separation; (2) whether the variables best separating the groups contain important information regarding the physiological nature of group difference; and (3) whether a composite, multivariate ‘discriminant function’ might be developed to serve as a potential biomarker [67] for CHR schizophrenia. In addition to gathering and analyzing resting EEG, a steady-state evoked potential, the frequency modulated evoked response (FMAER), was explored. The FMAER arises from the superior temporal (STG), bilaterally, and its use may facilitate physiological investigation of receptive language processing. The FMAER has shown abnormalities in children with a history of sudden-onset regressive autism [68, 69]. The STG is a site of interest having recently been suggested, by Fulham et al. [70], as a marker of abnormal functioning by ‘mismatch negativity’ in schizophrenia and prodrome, and by Oertel et al. [71, 72] as sources of auditory dysfunction in schizophrenia.

To obviate contamination by eye and or muscle artifact in the current study, a multi-step methodological approach was employed that was successfully used by the first author in the evaluation of group differences between children within the autism spectrum and CON subjects [35]. Furthermore, the full EEG analytic approach also

relies upon the computational reduction into a manageable number of factors of the large number of coherence and spectral variables produced by single subjects. This computational process facilitates an objective approach to data management for subsequent group analyses [73, 74]. It obviates the need for *a priori* preselection of a subset of coherence variables in order to avoid Type 1 and 2 statistical errors [74, 75].

Methods

Venue

All neurophysiological data collection and analysis was performed under the direction and supervision of the first author at the Developmental Neurophysiology Laboratory, Department of Neurology, Boston Children's Hospital (BCH), a university-affiliated (Harvard Medical School) academic medical center.

Subjects

Patients with Schizophrenia Prodrome Syndrome (CHR)

The CHR screening assessment included administration of the Schedule for Affective Disorders and Schizophrenia for School-Age Children-Present and Lifetime Version [76]; the K-SADS, as it is known, constitutes a validated semi-structured interview used to diagnose mood, anxiety, substance abuse, and psychotic disorders in youth under the age of 18. Both participant and parent/guardian report of the participant's symptom history were solicited for the current study.

A number of tests/indices have been devised in order to quantify identification and study of the CHR state [3, 77]. The current study employed the Scale of Prodromal Symptoms (SOPS) [78, 79]. The SOPS is embedded within an interview form, the Structured Interview for Prodromal Syndromes (SIPS), designed to diagnose prodromal (CHR) syndromes according to published criteria and to rate severity of CHR symptoms [19]. While the SIPS serves to define/identify the CHR state it does not in itself serve to identify later development of psychosis. The SIPS and the SOPS [80] were administered to all participants as part of the screening.

SIPS/SOPS raters were certified through a standard 1½-day training program developed by the assessment's creators at Yale University's PRIME Research Clinic. At the start of the current study, raters also attended the Boston site for the North American Prodromal Longitudinal Study (NAPLS-2) to study SIPS interview collection and scoring for 9 months to ensure consistent ratings across sites. Among the current study sample, 66 (97 %) of the SIPS/SOPS were performed by BCH staff; SIPS/SOPS scores for the remaining two participants were provided by their referral source, one from the NAPLS-2 and one from the Social Neuroscience and Psychopathology Laboratory

of Harvard University, as they had been assessed at these laboratories within 30 days of entering the current study.

In addition, information about past medical history, medication usage, school functioning, and academic functioning was obtained. The participant's parent/guardian and treating clinician were questioned to determine that the participant was functioning at grade level in a regular classroom without special education services and was without any other evidence of intellectual and/or academic disability. To further screen for academic and intellectual function outside normal range, the Scales of Independent Behavior-Revised was performed; this comprehensive scale constitutes a norm-referenced assessment of adaptive and maladaptive behaviors [81]. Only participants with positive SIPS/SOPS scores but without evidence of academic or intellectual disability were included in the current study.

On the day of the laboratory visit, the participant's parent/guardian completed a demographic questionnaire that asked for report of the participant's demographic information and medication usage. Parents/guardians were asked to provide consent for review of medical records to further characterize participants' mental health history. If more than 1 month had elapsed since the screening assessment, participants were re-administered the SIPS/SOPS to confirm that the participant remained within their previously determined clinical group. No participant was reclassified based upon reassessment.

Study subjects were recruited, under the direction of the senior author, from among three sources: clinical referrals to the BCH outpatient psychiatric clinic, the NAPLS-2 program, and the Social Neuroscience and Psychopathology Laboratory. Inclusion criteria were (1) a clinical diagnosis of 'schizophrenia prodromal (CHR) syndrome', including documentation by a senior staff psychiatrist of the patient's report of intermittent cognitive distortions (e.g. hallucinations, paranoia, delusions); (2) positive SOPS scores from the SIPS as administered by trained and certified technologists and confirmed by a staff psychiatrist; and (3) written agreement as required by the BCH Institutional Review Board (IRB) of the patient and/or parent/guardian to participate in the study. Exclusion criteria were the presence of any of the following: (1) co-existing primary neurologic syndromes (e.g. Trisomy X or Klienfelter's syndromes, tuberous sclerosis, traumatic brain injury, global developmental delay, developmental dysphasia, hydrocephalus, hemiparesis, or any other known syndromes affecting brain development); (2) coexisting primary psychiatric syndromes (e.g. depression, bipolar disorder, attention deficit hyperactivity disorder, obsessive-compulsive disorder); (3) clinical seizure disorders or results of prior EEG readings suggestive of an active seizure disorder or epileptic encephalopathy; (4) report of major medical illnesses (e.g. diabetes, severe asthma, cardiovascular abnormality, endocrine abnormality, etc.); (5) taking

prescription medication(s) at the time of study; or (6) significant primary sensory disorders (e.g. blindness and/or deafness).

Healthy, CON subjects

Healthy CON subjects were recruited by poster and colleague/acquaintance referral. None were recruited from within families of the subjects with schizophrenia prodrome syndrome. Controls were screened by the same procedure as described above for the CHR subjects. Inclusion criteria required (1) the absence of any symptoms of schizophrenia and (2) signed IRB consent as indicated above. Exclusion criteria were the presence of any of the following: (1) any neurological, psychiatric, and/or medical illnesses and/or primary sensory disorders, as for the CHR (prodrome) group spelled out above; (2) family history of schizophrenia or other major mental illness; (3) history of drug abuse; (4) non-specific 'suspicious' affect, appearance, or behavior as observed by the study personnel; or (5) taking prescription medication(s) at the time of study.

IRB approval

All subjects and/or their families, as age appropriate, gave written informed consent in accordance with protocols approved by the IRB of the BCH Office of Clinical Investigation. The approved protocol is in full compliance with the Helsinki declaration.

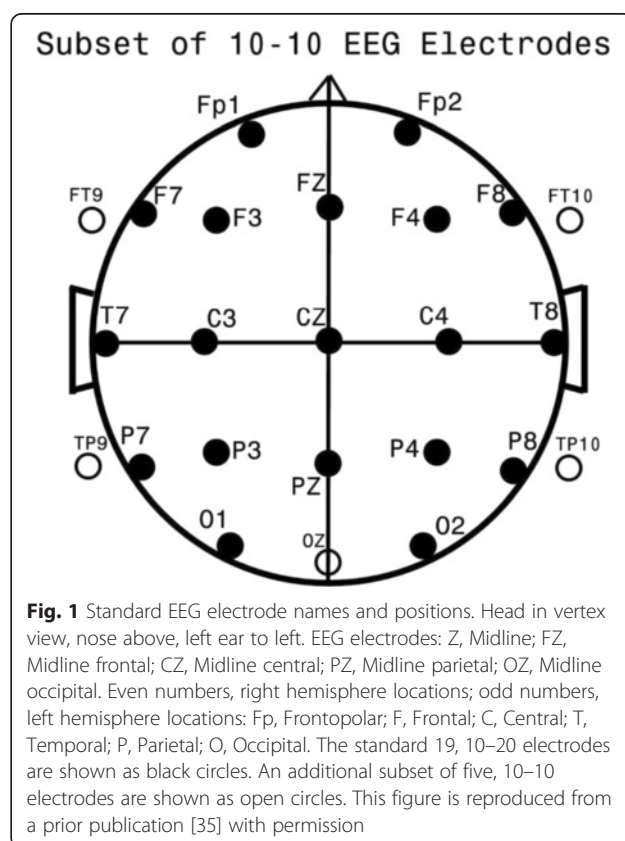
Data acquisition

Neurophysiology recording: EEG data collection and initial processing

All subjects' electrophysiological data obtained for this study were gathered by technologists trained and supervised by the first author, an experienced academic clinical electroencephalographer. Data were collected with an EGI™ 128 channel geodesic net system (Electrical Geodesics Inc., Eugene, OR, USA) along with a single information channel dedicated to a stimulus trial marker utilized for evoked potential collections (see FMAER below). A conductive gel rather than a salt solution was employed with the electrodes. Disadvantages of salt-soaked sponge electrode use include inter-electrode conductive 'salt bridges' and high electrode-scalp impedance due to more rapid drying out, both of which may lead to a difficult-to-detect increase in artifact. All subjects were studied in a sound and electronically (Faraday) shielded chamber and were visible and easily accessible to the technologist via one-way mirror window and door. The recording equipment stood outside of and immediately adjacent to the recording chamber. Data were sampled at 500 Hz with 0.1–100 Hz EEG band pass. Several separate epochs of eyes closed, waking state data were obtained over the course of the study with frequent breaks and verbal interchange to facilitate

alertness. Approximately a total of 20 minutes of apparently artifact-free waking EEG was recorded per subject. Eyes closed, waking state ambient EEG recordings were temporally interdigitated with sessions of evoked potential recordings (see below, FMAER). Frequent rest breaks were built in as indicated. After conclusion of data collection, all research subjects with electrode nets in place underwent photogrammetry with an 11 camera-based EGI system, so as to establish the precise position of the 128 net electrodes and thus to facilitate off-line mapping to standard EEG electrode positions for comparative purposes. Data were then de-artifacted (see below, Artifact management – part 1 and part 2), re-montaged by 3D spline interpolation, and signal averaged as indicated (FMAER) by BESA™ software (BESA GmbH, Gräfelfing, Germany). Original unprocessed data were permanently archived within a Developmental Neurophysiology Laboratory database.

For subsequent analysis, EEG, spectral, coherence, and FMAER data were additionally reduced in number by BESA using 3D spline interpolation to 24 standard EEG locations (FP1, FP2, F7, F3, FZ, F4, F8, T7, C3, CZ, C4, T8, P7, P3, PZ, P4, P8, O1, OZ, O2, FT9, FT10, TP9, TP10 – see Fig. 1 for standard EEG electrode placement), bandpass filtered from 0.5–50 Hz, mains filtered at 60 Hz, and down-sampled to 256 Hz so as to reduce data



dimensionality and facilitate comparison to data gathered with more common lower temporal and spatial resolution recording systems.

Neurophysiology recording: the Frequency Modulated Auditory Evoked Response (FMAER)

The FMAER stimulus was initially derived by Green and Stefanatos [82–86] as a means to assess the temporal lobes' ability to decode rapidly changing speech patterns, essential to the accurate detection of phonemes and, in turn, essential for language decoding and ultimately language comprehension. By means of source analysis the FMAER has been shown in neurotypical subjects to arise from both STG [68]. The FMAER is formed by starting with a 1000 Hz sine wave and frequency, modulating it with another 10 Hz sine wave, which results in 'warbling', and then further modulating it by slowly turning the warbling on and off with another 4 Hz sine wave [68]. A trial marker locked to the onset of one second of the 4 Hz sine wave and saved with concurrently recorded EEG produces, after signal averaging, a scalp recorded 4 Hz sine wave in normal subjects. The FMAER stimulus and trial marker are created by a stand-alone Spark2 generator (Mind Spark Inc., Newton, MA, USA). The auditory signal is bi-aurally presented by speakers at 78 db sound pressure level.

The FMAER response may be absent in the Landau-Kleffner syndrome when language deteriorates [64] and in autistic children with histories of rapid language and/or behavioral regression [65]. Successful pharmacologic treatment may improve receptive and expressive language function and restore a previously absent FMAER [64, 65]. FMAER spectral analysis has also shown that the FMAER scalp response may be as much 'distorted' as 'absent' in regressive autism associated with language loss [65].

Measurement issues and solutions: artifact management – part 1

After each subject's participation in the EEG study, EEG epochs were inspected by the EEG technologist to visually identify which epochs were recorded during breaks for relaxation, or showed movement artifact, electrode artifact, eye blink storms, drowsiness, epileptiform discharges, and/or bursts of muscle activity. When so identified, they were marked for exclusion from all subsequent analyses. The EEG technologist's results were reviewed for accuracy by the first author, who then removed remaining eye blink and eye movement artifacts, which may be surprisingly prominent even during the eyes closed state, by utilization of the source component technique [87–89] as implemented in BESA software. These combined techniques resulted in EEG data that appeared largely artifact free, with rare exceptions of low level temporal muscle artifact and persisting low voltage frontal and anterior temporal slow eye

movement, which however may contaminate subsequent analyses. The final reduction of any persisting contamination of processed variables (coherence) is discussed below under Artifact management – part 2.

Data processing

Calculation of spectral coherence and spectral variables

As previously described [35], 8–20 minutes of eyes closed, awake state EEG cycles per subject were transformed within BESA to the Laplacian or current source density reference. This approach provided reference-independent data that are primarily sensitive to underlying cortex and relatively insensitive to deep/remote EEG sources. Use of current source density reduces spurious effects of volume conduction upon coherence by emphasizing sources at small spatial scales [90].

Spectral coherence was calculated using a Nicolet™ (Nicolet Biomedical Inc., Madison, WI, USA) software package, according to the conventions recommended by van Drongelen [37, p. 143–4, equations 8.40, 8.44]. In practice, coherence is typically estimated by averaging over several epochs or frequency bands [37]. In the current project, a series of 2 second epochs was utilized to process available EEG segments. Spectral coherence measures were derived from the 1–32 Hz range, in 16 2-Hz-wide spectral bands resulting in 4,416 unique coherence variables. The 24 × 24 electrode coherence matrix yields coherence values where the matrix diagonal has a value of 1 – each electrode to itself – and half of the 552 remaining values duplicate the other half. This results in 276 unique coherences per spectral band. Multiplication by the 16 spectral bands in turn results in 4,416 unique spectral coherence values per subject [35].

Standard spectral data were calculated using the common average reference by FFT over the same frequency range noted above and based upon the FFT algorithm described in Press et al. [38, p. 411–2]. Resulting spectral data were utilized in order to approximate residual artifact contamination (see Artifact management – part 2) and as potential predictor variables. Per subject, the 24 EEG channels and 64 spectral bands per channel result in 1,536 spectral data values.

Measurement issues and solutions: artifact management – part 2

As previously detailed [35], visual inspection or direct elimination of electrodes and/or frequencies where a particular artifact is most easily apparent do not remove all artifact from an EEG data set on their own. An established approach to further reduce any persisting artifact contamination of processed coherence data involves multivariate regression. Semlitsch et al. [91] demonstrated that, after identifying a signal that is proportional to a known source of artifact, this signal's contribution to

scalp recorded data may be diminished by statistical regression procedures. As also previously detailed [35], persisting vertical eye movements and blinks produce slow EEG delta spectral signals in the frontopolar channels FP1 and FP2. Such artifact contribution may be estimated by the average of the 0.5 and 1.0 Hz spectral components from these channels after EEG spectral analysis by FFT of common average referenced data. Similarly, horizontal eye movements may be estimated by the average of the 0.5–1.0 Hz spectral components from anterior temporal electrodes F7 and F8. Little meaningful EEG information of brain origin is typically found at this slow frequency in these channels in the absence of extreme pathology. Muscle activity tends to peak at frequencies above those of current interest. Accordingly, 30–32 Hz spectral components were considered to be largely representative of muscle contamination, especially as recorded from the separate averages of prefrontal (FP1, FP2), anterior temporal (F7, F8), mid-temporal (T7, T8), and posterior temporal (P7, P8) electrodes. These electrodes are most often contaminated by muscle artifact as they are physically closest to the source of the artifact, namely the frontal and temporal muscles. The steps employed in the current study involved, first, the fitting of a linear regression model where the dependent variables were those targeted for artifact reduction and the independent variables were those chosen as representative of remaining artifacts; second, the extraction of the residuals, which now represented the targeted data after artifact removal; and, third, the use of the residuals in subsequent analyses. The six artifact measures, two very slow delta and four high frequency beta measures, were submitted as independent variables to a multiple regression analysis (BMDP2007™-6R) [92] in order to individually predict each of the coherence variables (see below), which were treated as the dependent variables. The residuals of the dependent variables, now uncorrelated with the chosen independent artifact variables, were used in the subsequent analyses. The above regressions were performed separately on both spectral and coherence data sets prior to principal components analysis (PCA; see below).

Prevention of capitalization upon chance: variable number reduction by creation of spectral and spectral coherence factors

Spectral and spectral coherence analyses produce many variables per subject. Steps must be taken to avoid capitalization on chance, which may result from the use of too many variables. Typically, the number of variables is reduced based upon expectations from results of prior analyses and/or current hypotheses. A more objective approach follows the advice of Bartels [73, 93], who proposed establishment of the intrinsic data structure within large data sets by use of PCA, and utilization of the resulting smaller set of computed factors to represent the

subjects in subsequent analyses. Modern texts continue to recommend PCA for variable reduction [94, 95]. Spectral and spectral coherence data were first normalized (centered and shifted to have unit variance) so that eventual factors reflect deviations from the average. The PCA-generated smaller set of factors that represents a large portion of the original variance results in a substantial reduction of the ultimate variable number per subject. This obviates the need for the ‘expert guided’ selection of variable subsets for subsequent statistical analyses with resulting risk of type 1 and type 2 statistical error. A data set of uncorrelated (orthogonal) factors is produced in which a small number of orthogonal factors are identified following varimax rotation.

Each factor is formed as linear combination of all input variables with the weight or loading of each coherence variable upon a particular factor as determined by the PCA computation [73]. Meaning of outcome factors is discerned by inspection of the loadings of the input variables upon each individual factor [73, 96]. Factor loadings were treated as if they were primary neurophysiologic data and displayed topographically [97, 98]. A display of approximately the highest 15 % of coherence loading values was utilized to facilitate an understanding of individual factors’ meaning (Figs. 2 and 3). This approach has been used successfully for both spectral [99] and spectral coherence [35, 100–102] data reduction and analysis.

FMAER: spectral signal and noise analysis

As described above, a normal subject’s 4 Hz FMAER appears, upon scalp recording, in the form of a one second 4 Hz sine wave. Abnormal FMAERs – as observed in some children with Landau-Kleffner syndrome or autism – appear as noisy, distorted, or partial 4 Hz sine wave, or occasionally just as low amplitude noise [68, 69]. ‘Noisy’ responses may reflect four possibilities: (1) there is no 4 Hz response and the noise reflects residua of incomplete signal averaging; (2) a low amplitude 4 Hz response is present but is partially masked by noise from incomplete averaging; (3) the response itself is distorted, causing a non-sinusoidal appearance (side-band noise); or (4) a combination of these possibilities. A study of children with regressive autism using spectral analysis of FMAERs formed from both standard averaging and ‘plus-minus’ averaging [37] demonstrated that, at baseline, children with absent language demonstrated FMAERs manifesting distorted processing, i.e. the 4 Hz auditory input to the ears produced, instead of a clean 4 Hz scalp sinusoid, a broad-band 2–7 Hz response [69]. Accordingly, spectral analysis was performed on the current study subjects’ FMAERs in order to search for evidence of auditory processing distortion in schizophrenia prodrome. FFTs were formed on all subjects in the current populations at 4 Hz (response frequency) as well at 3 Hz and 5 Hz (sideband noise frequencies).

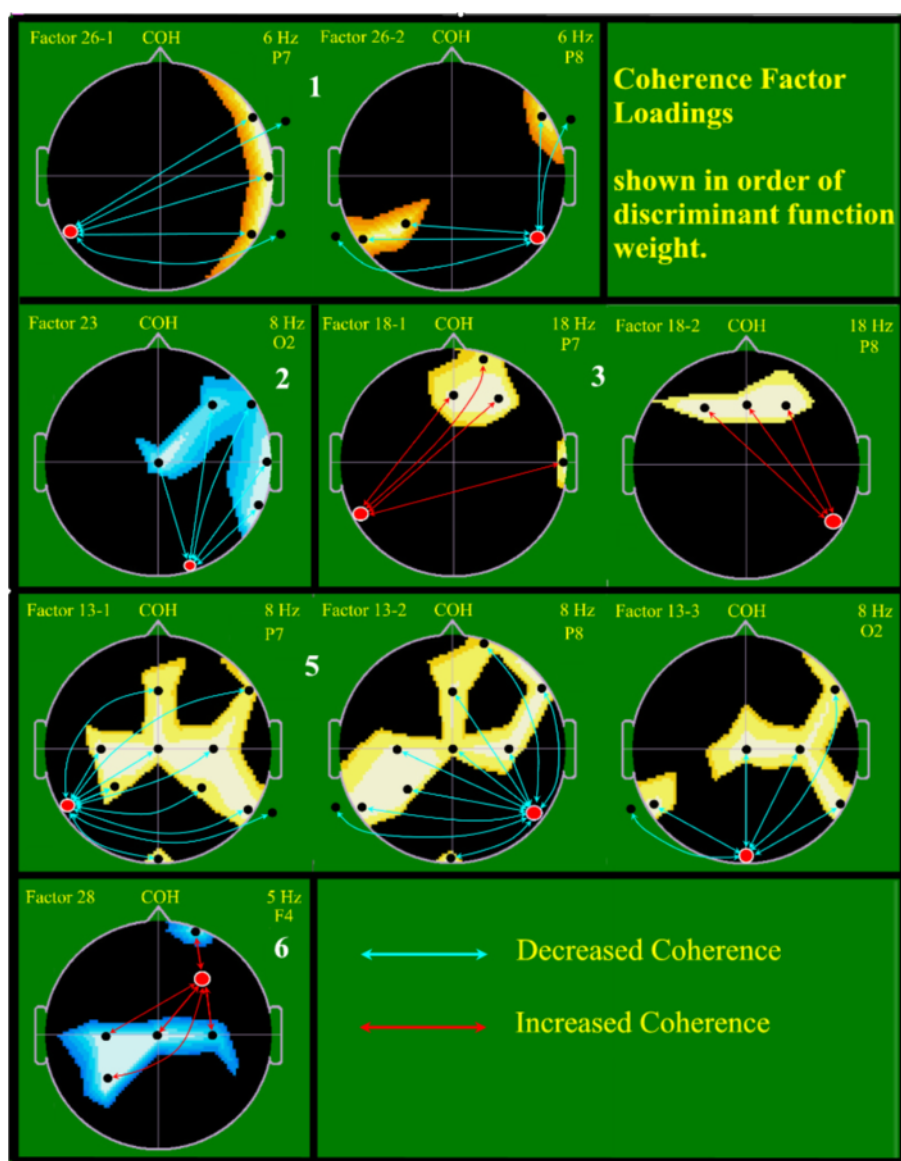


Fig. 2 Factor loadings for five coherence factors chosen to best differentiate clinically high risk (CHR) from neurotypical controls. Schematic heads are shown in vertex view, scalp left to image left with nose above. Each one of the five black-bordered rectangles or squares displays, within its borders, information relevant to a single one of the five coherence factors selected by discriminant function analysis (DFA; see text). For example, the first row displays data describing the first factor chosen by DFA, Factor 26. Factor name is shown above and to the left of each image (e.g. Factor 28), in yellow. Above the nose 'COH' indicates that the image displayed is a coherence factor. Where a factor requires more than one image to illustrate relevant coherence loadings, they are separately labeled (e.g. Factor 26–1, Factor 26–2). The order of selection by DFA for each coherence factor within the overall choice of eight factors is shown as a large white number. To the top right of each image is the relevant spectral frequency and primary index electrode, displayed in yellow (e.g. 6 Hz P7). The colored regions within the images reflect the region and sign of coherence loadings from the initial PCA. The index electrode for each image is shown as a red circle bordered in white. Lines connect this index electrode to additional electrodes (black dots). Line color reflects reduced (blue) or increased (red) coherence for the CHR population

Data analysis

Discrimination of subject groups by use of EEG spectral coherence and spectral variables

Two-group DFA [96, 103, 104] was used in the current study. As previously described [35], it produces a new canonical discriminant variable which maximally separates

the groups based on a weighted combination of the entered variables. DFA defines the significance of a group separation, summarizes the classification of each subject, and provides approaches to the prospective subjective classification by means of the jackknifing technique [105–107]. The BMDP statistical package [108] was employed for

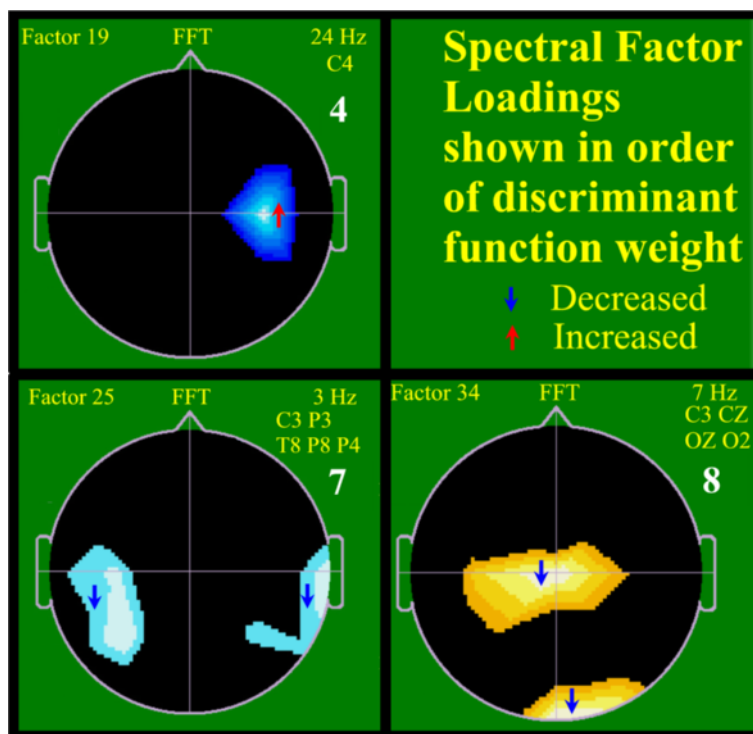


Fig. 3 Factor loadings for three spectral factors chosen to best differentiate clinically high risk (CHR) from neurotypical controls. Schematic heads are shown as for Fig. 2. Each of the three black-bordered squares displays information relevant to one of the three spectral factors selected by discriminant function analysis (DFA; see text). Above the nose “FFT” signifies the image displayed is a spectral factor. Relevant spectral bands and electrodes are shown above and to the right. The order of selection by DFA for each spectral factor within the overall choice of eight factors is shown as a large white number. For example, the first square displays data for FFT Factor 19 involving 24-Hz activity at electrode C4 and was the fourth factor chosen by DFA. The colored regions within the images reflect the region and sign of spectral loadings from the initial PCA. Color of a small associated arrow reflects reduced (blue) or increased (red) spectral activity for the CHR population

DFA (program 7 M) which yields the Wilks’ Lambda statistic with Rao’s approximation. For the estimation of prospective classification success, the jackknifing technique was used [105–107] as provided within program 7 M. In jackknifing for two-group DFA, the discriminant function is formed on all subjects but one. The left-out subject is subsequently classified. This initial left-out subject is then folded back into the group (hence “jackknifing”), another subject is left out, the DFA is performed again, and the newly left-out subject classified. This process is repeated until each individual subject has been left out and classified on the basis of the ‘non-left-out’ subjects. The assessment of prospective classification success is based upon a tally of the left out subjects’ correct classification. This technique is also referred to as the ‘leaving-one-out’ process and is generally taken as an estimate of future classification success for populations of the size used in this project. A better estimation of classification success involves multiple split-half replications as previously demonstrated on a large population of autistic children [35]. It is notable that, within the autism study the group, the average split half classification success and the corresponding jackknifed classification were quite comparable.

Results

Subjects

Over the past 4 years, 35 CON subjects were recruited and 57 putative patients with CHR were identified. Twenty of the 57 manifested psychosis and an additional 15, although non-psychotic, had been placed on medications by the time of neurophysiologic evaluation. Accordingly, these 35 were excluded from the study target sample of unmedicated patients with CHR. The remaining 22 non-psychotic, unmedicated CHR patients made up the population to be contrasted with the CON group. The final data analyses were, therefore, based upon 35 control subjects and 22 subjects with unmedicated CHR. Relevant, selected CON and CHR group demographics are shown in Table 1.

EEG data were collected on the full population of 92 subjects and all were utilized for the purpose of coherence and spectral variable reduction by PCA so as to maximize the information/variance content within the PCA analyzed data set.

There were no significant differences between the CON and CHR groups in terms of handedness and sex. Significant difference in mean age between these two groups was managed by removing the effect of age upon variables,

Table 1 Control and high risk population demographics

Variable	Controls n = 35	Behavioral high risk n = 22	Fisher exact test
Sex	14 males 21 females	11 males 11 females	n/s
Handedness	34 right 1 left	20 right 2 left	n/s
		Mean ± SD	
Age at study	19.175 ± 5.690	13.679 ± 3.240	T-test = 4.04; P ≤ 0.0002

n, group population size; n/s, not statistically significant; P, probability

prior to use in discriminant analysis, using statistical regression.

Factor development by PCA

Data reduction (factor formation) was independently performed for the 4,416 spectral coherence variables and the 1,536 spectral variables. For PCA on the coherence data, results demonstrated, after varimax rotation, a good condensation of variance upon a small number of factors. After varimax rotation, the first coherence factor accounted for 2.98 % of the total variance contained within the full set of the original 4,416 coherence variables. Five factors accounted for 15.14 % of the original variance, and the full 40 factors accounted for 77.82 % of the overall variance. For PCA on the spectral data, results demonstrated even stronger data condensation. After varimax rotation the first spectral factor accounted for 14.13 % of the total original variance, five factors accounted for 44.07 % of the variance, and the full 40 factors accounted for 95.92 % of the total, original variance. Age at study was regressed (BMDP-6R) from all factors before use in subsequent analyses. Loadings of original coherence and spectral variables upon corresponding summary factors are illustrated in Figs. 2 and 3.

Discriminant function analysis (DFA)

Two-group stepwise discriminant function analysis (BMDP 7 M) was instituted contrasting groups CON (n = 35) and CHR (n = 22), where coherence and spectral factors were allowed to enter (F to enter 4.0, to remove 3.996). Results are shown in Table 2. As evident, the F statistic approximation to Wilks' Lambda was statistically significant (P ≤ 0.00001). Five coherence and three spectral factors were utilized (Table 3). The first three variables chosen and five of the eight chosen variables were coherence factors. Initial classification was 91.2 % correct overall (CON, 88.6 %; CHR, 95.5 % correct). The classification success upon completion of jackknifing was 86.0 % correct overall (CON, 85.7 %; CHR, 86.4 % correct). The groups were displayed as a histogram on the canonical discriminant variable (generated from the eight chosen factors) showing a mostly bimodal distribution (Fig. 4).

Table 2 Discriminant function analysis controls (CON) vs. clinical high risk (CHR)

(1) Standard analysis			
Group	Percent	Number of subjects classified	
	Correct	CON	CHR
CON	88.6	31	4
CHR	95.5	1	21
TOTAL	91.2		
(2) Jackknife analysis			
Group	Percent	Number of subjects classified	
	Correct	CON	CHR
CON	85.7	30	5
CHR	86.4	3	19
TOTAL	86.0		
(3) Eight factors chosen to make discrimination, in order of choice			
		Overall estimated significance	
1. COH 26	Wilk's lambda = 0.419		
2. COH 23	DF = 8, 48	F = 8.313	p = 0.00001
3. COH 18			
4. FFT 19			
5. COH 13			
6. COH 28			
7. FFT 25			
8. FFT 34			

COH, Coherence factor; FFT, Spectral factor; DF, Degrees of freedom for F test; F, F statistic; P, Estimated probability

Factor loadings

Figure 1 illustrates the standard placement for the 24 EEG electrode locations utilized, whereas Figs. 2 and 3 illustrate the loading patterns for the five chosen coherence factors and for the three chosen spectral factors, respectively, as utilized in the above DFA. Three of the five coherence factors involved numerous coherence loadings and, for the purpose of clarity, more than one image was utilized

Table 3 Sample frequency modulated auditory evoked response (FMAER) scores

Variable	Mean ± SD		
	Controls	High risk	Probability
3 Hz-TP9	0.0331 ± 0.102	0.0301 ± 0.055	n/s
4 Hz-TP9	0.6892 ± 1.707	0.5471 ± 0.584	n/s
5 Hz-TP9	0.0456 ± 0.014	0.1441 ± 0.039	n/s
3 Hz-TP10	0.0022 ± 0.055	0.0407 ± 0.058	n/s
4 Hz-TP10	0.8177 ± 0.531	0.9479 ± 0.708	n/s
5 Hz-TP10	0.0539 ± 0.008	0.1231 ± 0.027	n/s

4 Hz, Targeted signal frequency; 3 Hz, 5 Hz, Side band frequencies; TP9, TP10, Respective left and right posterior temporal regions, expected sites of maximum left and right sided FMAER response (typical FMAER waveforms, normal and abnormal, may be viewed in on-line references [64, 65]); n/s, Not significant by Student's t-test

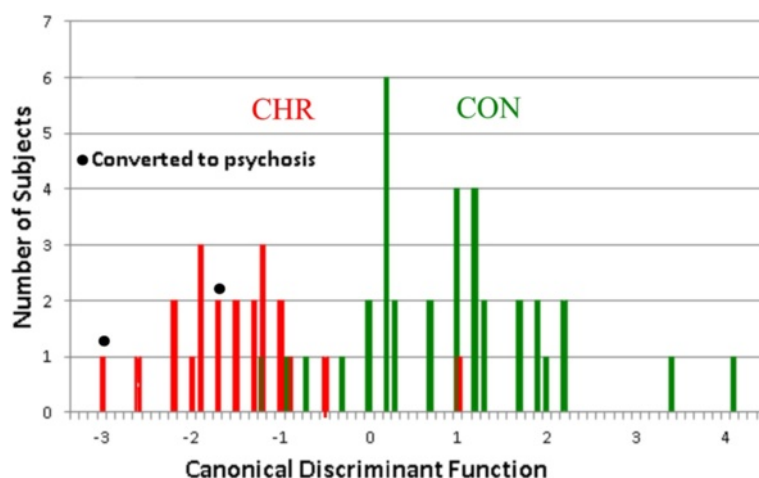


Fig. 4 Clinical high risk (CHR) and neurotypical control (CON) population distributions on the discriminant function analysis-derived canonical discriminant variable. Population distributions are shown for the CON (green) and CHR (red) groups. The X axis is the canonical discriminant, ranging from +4.5 to -3.5 units, which was created by the DFA process utilizing the eight factors described in Table 2, part (3). The Y axis represents subject number

for demonstration, e.g. the first coherence Factor 13 is depicted in three separate images. Each image is shown in vertex view, i.e. from above; the left ear is shown to the left and the nose above.

In each coherence factor image the index electrode and primary EEG frequency are named top right and the referenced electrode is also shown in red with a white circle. Blue or red lines with arrow tips indicate the other involved electrode (black circle) for each involved coherence pair. Blue lines indicate reduced coherence for the CHR group and red lines indicate increased coherence for the CHR group in the featured DFA. Three coherence factors demonstrated reduced coherence (Fac 26, 23, 13) and two increased coherence (Fac 18, 28). Note that the first two chosen factors manifest reduced coherence. Thus, although both reduced and increased coherence are observed, reduced coherence predominates. Also note, in Fig. 2, that long distance coherence (coherence other than to adjacent electrode) predominates. No single coherence factor demonstrated a combination of decreased and increased factor loadings. Four coherence factors involved both hemispheres (Fac 26, 18, 13, 28) and one factor just involved the right hemisphere (Fac 23). Involved spectral bands were limited to the theta (Fac 26, 23, 13, 28) and slow beta (Fac 18) spectral bands.

The colored background in the illustrated coherence factors indicates the coherence loading from the original PCA which, in combination with the loading of the PCA-produced factors on the discriminant canonical variable, determines the color of the lines (red or blue, see below). Regions involved by coherence factor index electrodes (red, white circle) are temporal – six (within Fac 26, 18, 13), occipital – two (Fac 23, 13), and frontal – one

(Fac 28). Of the six temporal index electrodes, all involved the posterior temporal regions, three left and three right sided. All six coherence factors involved primarily long distance associations. None involved predominantly short distance associations.

For each of the three spectral (FFT) factors used in the DFA, regions involved are illustrated in color, which reflects loading of the regions’ spectral content upon the given factor in the PCA. Next to each region is a small arrow, the color and direction of which reflects spectral change for the CHR group in the DFA (red, up, increase for CHR group; blue, down, reduction in CHR group). Just one factor demonstrated increased CHR spectral magnitude (Fac 19) and two manifested decreased magnitude (Fac 25, 34). All spectral factors reflected one single spectral band: delta (Fac 25), theta (Fac 34), and beta (Fac 19). Areas involved by the spectral factors included the central-parietal (Fac 4, 25, 34), temporal (Fac 25), and occipital (Fac 34) regions. None of these regions are typically associated with eye or muscle artifact.

FMAER data analysis

The FMAER paradigm was performed on the 35 CON and 22 CHR subjects. A standard average was created as well as a plus-minus average. The former creates an average combination of the signal response, average of noise within the response, and residual background noise left after averaging. The latter produces an estimate of the residual background noise left after averaging [37, p. 61]. Both the standard and the plus-minus average response were spectral analyzed by BESA from 3 through 5 Hz across all 24 channels utilizing the common average reference. Subtraction of spectral analysis of the plus-minus

average from that of the standard average created a spectral difference plot where random background noise is removed but the response remains. Ideally, the 3 Hz and 5 Hz sideband spectral values should be zero and the 4 Hz component should be prominent. When the subtracted values for the groups were compared by Student's t-test, no significant differences were observed for any frequency or electrode. Table 1 shows the results for the bilateral posterior-inferior temporal electrodes TP9 and TP10 (Fig. 1), electrodes that typically reflect maximal FMAER scalp amplitude [64, 65]. Thus, there was no FMAER evidence for any difference in response (at 4 Hz) magnitude or response distortion (at 3 or 5 Hz) between the CHR and the CON group at the two electrodes typically showing greatest response amplitude [68, 69]. Note the large difference in mean magnitude between the 4 Hz signal and the adjacent 3 and 5 Hz sideband noise components for both studied groups. In other words, both groups manifested normally appearing FMAER responses.

Table 4 illustrates the expected large SOPS scores differences between the CON and CHR groups.

Discussion

The objectives of the present study included the development of neurophysiological descriptors of schizophrenia prodrome (CHR) derived from ambient resting EEG. The descriptors were expected to fulfill a series of criteria, included (1) freedom from artifact contamination; (2) being objective and bias free; (3) useful in the quantitative classification/identification of schizophrenia prodrome (CHR); (4) useful in creation of putative, quantitative biomarker for CHR; (5) clinically interpretable; and (6) facilitating assessment of the functional integrity of the STG.

First, although infrequently emphasized, artifact may significantly interfere with group study results that involve quantification of EEG. Excessive artifact adds noise, thereby obscuring discovery of significant group differences (type 2

statistical error, false negatives), or presents asymmetrically within one group causing a spurious group difference (type 1 error, false positives). In order to obviate or at least minimize such possibilities, a four-part process was undertaken. Initially, prominent artifact containing EEG segments were removed by expert visual inspection of EEG. Then, eye blink was computationally eliminated by a source analysis technique [87–89]. Next, small residua of eye movement and muscle were removed by a regression technique [91]. Finally, higher frequencies above 30 Hz (gamma band) were excluded from analysis, in agreement with literature suggesting that such gamma activity is strongly dominated by cranial muscle activity [61]. As a result of the above process, factor loading patterns do not suggest artifactual origins. Moreover, the statistical regression assures that utilized variables are 'artifact free', i.e. statistically uncorrelated with (orthogonal to) quantitative estimates of artifact sources.

Second, as originally proposed by Bartels [73, 93], and subsequently refined for use with neurophysiological data [74] and utilized in this laboratory [35, 74, 100, 102], PCA constitutes an objective way to demonstrate the fundamental structure within a data set and simultaneously an objective way to reduce variable number without need for a priori intervention. In this study of coherence data, 40 factors represented 78 % of the information (variance) within the 4,416 original spectral coherence variables per subject. For spectral data, 40 factors represented 96 % of the information within the 1,536 variables per subject. This constitutes a substantial, unbiased reduction of data dimensionality for both spectral and coherence data sets. The high retention of variance indicates that, while reducing data dimensionality, the PCA process preserved the majority of information contained within the original data set variables.

Third, stepwise discriminant analysis (DFA) between the CON and prodrome (CHR) groups demonstrated successful group separation with 91 % correct initial subject classification. This was done on the basis of eight variables, yielding a favorable subject to variable ratio of 57/8, approximately 7:1 [109]. More importantly, jackknifing [105, 106] demonstrated 86 % correct classification for both groups, a favorable indicator [103, 110] for the prospective 'diagnostic utility' of EEG derived spectral and coherence data.

Fourth, the DFA canonical discriminant function variable graph (Fig. 4) showed a bimodal distribution between the CON and CHR. This raises the possibility that such a composite univariate discriminant variable formed on larger populations might serve to facilitate identification of response to intervention and/or subsequent conversion to schizophrenia. For example, it is speculated that a given CHR intervention appearing to have little or no positive clinical effect might, in fact, move a subject or subjects

Table 4 Structured Interview for Prodromal Syndromes (SIPS) – Scale of Prodromal Symptoms (SOPS) scores

Variable	Mean ± SD		T-test	Probability
	Controls	High risk		
P _{MAX}	0.486 ± 0.781	4.333 ± 0.658	19.720	0.0000
P _{AVG}	0.177 ± 0.177	2.429 ± 0.985	10.020	0.0000
N _{MAX}	0.114 ± 0.323	1.875 ± 0.409	7.680	0.0000
N _{AVG}	0.033 ± 0.017	1.395 ± 0.304	5.880	0.0000
D _{MAX}	0.200 ± 0.531	2.810 ± 0.273	9.090	0.0000
D _{AVG}	0.071 ± 0.215	1.202 ± 0.835	6.090	0.0000
G _{MAX}	0.171 ± 0.514	3.381 ± 1.600	8.940	0.0000
G _{AVG}	0.057 ± 0.172	2.131 ± 1.264	7.480	0.0000

P, positive symptoms; N, negative symptoms; D, disorganized symptoms; G, general symptoms; MAX, maximum of six scale scores per symptom type, per subject; AVG, average of six scale scores per symptom type, per subject

along the EEG discriminant from the CHR towards the CON region. Perhaps combinations of such apparently clinically silent, but favorably EEG active, interventions might in aggregate prove to be of combined clinical value. To facilitate the above, PCA and DFA analyses performed for this study allow new subjects (or subjects before and after intervention) to be passed through factor formation and discriminant classification.

Fifth, factor loading plots (Figs. 2 and 3) showed coherence patterns determined by the intrinsic data structure and did not manifest the typical, orderly left-right inter-hemispheric and anterior-posterior intra-hemispheric coherence patterns often pre-selected for analysis. Index coherence electrodes were mostly located over temporal lobes, predominantly involving the posterior temporal regions. Next, most prominent were occipital and frontal index electrodes. Although factors representing both decreased and increased coherence were observed, reduced coherence predominated, with long distance coherence patterns prevailing. From the seven DFA-selected spectral factor plots, none involved the prefrontal and only one the temporal region suggesting successful avoidance, or at least minimization, of spurious artifact dominated variables [40–42].

In agreement with many studies suggesting temporal lobe abnormalities in schizophrenia [33, 71, 72, 111–119] and schizophrenia prodrome [33, 112, 113], the current coherence findings strongly implicate the bilateral temporal areas. Reduced posterior temporal connectivity might be relevant in terms of the complex language disorders in schizophrenia [120] that presumably extend as well to CHR [121]. Our coherence findings are also in line with the studies of Oertel-Knöchel et al. [71, 72], who found functional MRI (fMRI) evidence of reduced connectivity with the planum temporale and the STG within schizophrenics and close relatives. These authors speculated that such findings might be associated with psychotic symptoms, especially auditory hallucinations. Moreover, Mou et al. [122] showed that schizophrenics who report auditory verbal hallucinations and who also demonstrated measured deficits in voice identity recognition, manifest impaired frontal-temporal connectivity. The current study's coherence factors 18, 13, and possibly 28 may be consistent with such altered frontal-temporal connectivity. In addition, the current findings of mixed but predominantly widespread reduced coherence in the awake resting state contradict prior speculations that increased coherence presents a primary schizophrenia biomarker [46].

In contrast to the current study's coherence findings implicating reduced connectivity with both posterior temporal regions, the FMAER data demonstrate normal primary receptive auditory processing in the cortex of both STG. This finding stands in contrast with earlier reports, as summarized in Methods, that in some patients

with the Landau-Kleffner syndrome [68] and regressive autism [69], the FMAER may be absent and/or distorted. A likely interpretation of the current results is that, in CHR, there is normal initial/early cortical processing of the auditory inputs within the STG but that the STG regions manifest impaired connectivity with other cortical areas that are broadly important in higher level language processing. Putative auditory processing dysfunction in CHR may depend more upon altered access of other regions to the posterior temporal regions and less on language processing within the STG itself – where, in contrast, the defects appear to exist in Landau-Kleffner syndrome and regressive autism.

Our findings of widespread alteration of cortical connectivity in schizophrenia prodrome augment recent findings in animal models of schizophrenia that emphasize abnormalities of functional interactions among various thalamic, frontal, and temporal regions [123–125]. Although progress has been made in avoidance of eye and muscle contamination within quantitative EEG studies, there remain fundamental issues with cleanly accessing and quantifying 'true' brain generated delta and gamma band signals that appear most relevant in animal studies which record directly from brain. The process of scalp EEG artifact avoidance no doubt diminishes or degrades true brain delta and gamma signals. Accordingly, current findings cannot exclude potentially relevant delta and gamma coherence differences in CHR. However, current data provide robust indications of a statistically significant CHR cortical difference in CHR at frequencies outside the delta and gamma bands. More work needs to be performed to obviate continuing technical hurdles in processing scalp-recorded EEG.

It must also be emphasized that EEG-based evidence of altered cortical connectivity in CHR should not be considered causal per se. The origins of CHR are likely to involve environmental, developmental, anatomical, genetic, and/or neurochemical factors yet to be conclusively elucidated. Such factors may bring about the behavioral syndrome known as CHR and its associated, potentially identifying, EEG coherence changes.

Conclusion

This study constitutes a demonstration that, following careful artifact management and objective variable number reduction while maximizing information retention, waking EEG significantly separates patients with CHR (prodromal) schizophrenia from neurotypical controls. The importance of these results rests partly on the relative simplicity and low cost nature of ambient awake EEG data recordings in comparison to the higher cost and complexity of MRI and fMRI data collection processes.

It is also to be noted that EEG data, including passive, specialized auditory stimulation (FMAER), provide additional information – when processed as show above – that

augment fMRI-based findings. Current data reinforce prior fMRI findings of temporal lobe dysfunction in schizophrenia. Current EEG data further suggest that auditory hallucinations and auditory processing abnormalities may indeed reflect abnormal connectivity with the posterior temporal lobes but not with associated auditory processing dysfunction within the bilateral superior temporal gyri themselves.

In addition to successfully classifying individual subjects, the canonical discriminant function might also serve as a quantitative biomarker. It is speculated that potentially useful therapeutic interventions might be identified by their effectiveness in moving individual subjects from their initial position along the canonical (biomarker) axis (Fig. 4) as determined by a pre-treatment study, towards the neurotypical end of the axis on the basis of a second post-treatment study following therapeutic intervention. Furthermore, it is speculated that the initial position along the biomarker axis might serve to identify those subjects with prodrome syndrome who are destined to convert to full psychosis/schizophrenia.

However, further studies on larger populations will be required to confirm the demonstrated classification success as well as to establish these hypothetical possibilities regarding use of the discriminant function as a scaled biomarker.

Abbreviations

BCH: Children's Hospital Boston; CHR: Schizophrenia prodrome syndrome (clinical high risk) group; CON: Neurotypical control subject group; DFA: Discriminant function analysis; EEG: Electroencephalogram; Fac: Factor, from PCA; FFT: Fast Fourier transform, used for spectral analysis; FMAER: Frequency modulated auditory evoked response; fMRI: functional MRI; iGBR: induced gamma-band EEG response; IRB: Institutional review board; MRI: Magnetic resonance imaging; n/s: not statistically significant; NAPLS-2: Boston site for the North American Prodromal Longitudinal Study; PCA: Principal components analysis; SIPS: Structured Interview for Prodromal Syndromes; SOPS: Scale of Prodromal Symptoms; STG: Superior temporal gyrus/gyri.

Competing interests

The authors declare that they have no competing interests.

Authors' contributions

Study concept and design, all authors; selection of patients and subjects, JG; acquisition and preparation of neurophysiologic data and statistical analyses, FHD; interpretation of results, FHD, AR, JG. JG and ED had full access to all the SIPS/SOPS data and take full responsibility for accuracy of subject selection. FHD had full access to all the neurophysiologic data in the study and takes responsibility for all aspects of these data including collection, processing, and analyses. All authors collaborated in writing and editing the paper and approved the final manuscript.

Authors' information

FHD is a physician, child neurologist, electroencephalographer, neurophysiologist and epileptologist with undergraduate degrees in electrical engineering and mathematics. Current research interests are in neurodevelopmental disorders (including schizophrenia) and the development and utilization of specialized techniques to support related investigations. ED is a clinical child and adolescent psychologist and clinical researcher with an interest in developmental risk for schizophrenia. AR is a physician, child neurologist, epileptologist, electroencephalographer, and clinical and research neurophysiologist. Research interests include transcranial magnetic stimulation and its application to epilepsy and

neurodevelopmental disorders. JG is a physician, child psychiatrist, and clinical researcher with interest in neurodevelopmental disorders and the development of schizophrenia.

Acknowledgements

The authors thank all subjects and their families who participated in the studies performed. They further thank technologists who performed the selection testing, ran the data collection procedures, and assisted in the data analyses: Sarah Gumlak, April Kim, Kara Kimball, Kyle O'Donnell, Ashley Rober, and Sahil Tembulkar. Heidelise Als, PhD, is thanked for her critical review of the manuscript. This project was primarily supported by a grant from the Tommy Fuss Foundation (Joseph Gonzalez-Heydrich, principal investigator) and the BCH departments of Psychiatry (David DeMaso, chairperson) and Neurology (Scott Pomeroy, chairperson). Additional support was received from the Intellectual and Developmental Disabilities Research Center grant HD018655 to Scott Pomeroy, MD.

Author details

¹Department of Neurology, Boston Children's Hospital and Harvard Medical School, 300 Longwood Ave, Boston, Massachusetts 02115, USA. ²Department of Psychiatry, Boston Children's Hospital and Harvard Medical School, 300 Longwood Ave, Boston, Massachusetts 02115, USA.

Received: 7 May 2015 Accepted: 19 October 2015

Published online: 02 November 2015

References

- Saha S, Whiteford H, McGrath J. Modelling the incidence and mortality of psychotic disorders: data from the second Australian national survey of psychosis. *Aust N Z J Psychiatry*. 2014;48(4):352–9.
- Hogerzeil SJ, van Hemert AM, Rosendaal FR, Susser E, Hoek HW. Direct comparison of first-contact versus longitudinal register-based case finding in the same population: early evidence that the incidence of schizophrenia may be three times higher than commonly reported. *Psychol Med*. 2014;44(16):3481–90.
- Larson MK, Walker EF, Compton MT. Early signs, diagnosis and therapeutics of the prodromal phase of schizophrenia and related psychotic disorders. *Expert Rev Neurother*. 2010;10(8):1347–59.
- Bera RB. Patient outcomes within schizophrenia treatment: a look at the role of long-acting injectable antipsychotics. *J Clin Psychiatry*. 2014;75 Suppl 2:30–3.
- Quarantelli M, Palladino O, Prinster A. Patients with poor response to antipsychotics have a more severe pattern of frontal atrophy: a voxel-based morphometry study of treatment resistance in schizophrenia. *Biomed Res Int*. 2014;2014:325052.
- Lysaker PH, Roe D, Buck KD. Recovery and wellness amidst schizophrenia: definitions, evidence, and the implications for clinical practice. *J Am Psychiatr Nurses Assoc*. 2010;16:36–42.
- Silverstein SM, Bellack AS. A scientific agenda for the concept of recovery as it applies to schizophrenia. *Clin Psychol Rev*. 2008;28(7):1108–24.
- Harrow M, Jobe TH. How frequent is chronic multiyear delusional activity and recovery in schizophrenia: a 20-year multi-follow-up. *Schizophr Bull*. 2010;36(1):192–204.
- Murray RM, Lewis SW. Is schizophrenia a neurodevelopmental disorder? *Br Med J*. 1987;295:538–55.
- Walker E, Lewis N, Loewy R, Palyo S. Motor dysfunction and risk for schizophrenia. *Dev Psychopathol*. 1999;11(3):509–23.
- Walker EF. Developmentally moderated expressions of the neuropathology underlying schizophrenia. *Schizophr Bull*. 1994;20(3):453–80.
- Schenkel LS, Silverstein SM. Dimensions of premorbid functioning in schizophrenia: a review of neuromotor, cognitive, social, and behavioral domains. *Genet Soc Gen Psychol Monogr*. 2004;130(3):241–70.
- Munro JC, Russell AJ, Murray RM, Kerwin RW, Jones PB. IQ in childhood psychiatric attendees predicts outcome of later schizophrenia at 21 year follow-up. *Acta Psychiatr Scand*. 2002;106(2):139–42.
- Davidson M, Reichenberg A, Rabinowitz J, Weiser M, Kaplan Z, Mark M. Behavioral and intellectual markers for schizophrenia in apparently healthy male adolescents. *Am J Psychiatry*. 1999;156(9):1328–35.
- Zipursky RB, Christensen BK, Mikulis DJ. Stable deficits in gray matter volumes following a first episode of schizophrenia. *Schizophr Res*. 2004;71(2–3):515–6.

16. Olsen KA, Rosenbaum B. Prospective investigations of the prodromal state of schizophrenia: review of studies. *Acta Psychiatr Scand*. 2006;113(4):247–72.
17. Cadenhead KS. Vulnerability markers in the schizophrenia spectrum: implications for phenomenology, genetics, and the identification of the schizophrenia prodrome. *Psychiatr Clin North Am*. 2002;25(4):837–53.
18. Mason O, Startup M, Halpin S, Schall U, Conrad A, Carr V. Risk factors for transition to first episode psychosis among individuals with 'at-risk mental states'. *Schizophr Res*. 2004;71(2–3):227–37.
19. McGlashan TH, Zipursky RB, Perkins D, Addington J, Miller TJ, Woods SW, et al. The PRIME North America randomized double-blind clinical trial of olanzapine versus placebo in patients at risk of being prodromally symptomatic for psychosis. I. Study rationale and design. *Schizophr Res*. 2003;61(1):7–18.
20. Miller TJ, McGlashan TH, Rosen JL, Cadenhead K, Cannon T, Ventura J, et al. Prodromal assessment with the structured interview for prodromal syndromes and the scale of prodromal symptoms: predictive validity, interrater reliability, and training to reliability. *Schizophr Bull*. 2003;29(4):703–15.
21. Morrison AP, French P, Walford L, Lewis SW, Kilcommons A, Green J, et al. Cognitive therapy for the prevention of psychosis in people at ultra-high risk: randomised controlled trial. *Br J Psychiatry*. 2004;185:291–7.
22. Nieman DH, Rike WH, Becker HE, Dingemans PM, van Amelsvoort TA, de Haan L, et al. Prescription of antipsychotic medication to patients at ultra high risk of developing psychosis. *Int Clin Psychopharmacol*. 2009;24(4):223–8.
23. Manninen M, Lindgren M, Therman S, Huttunen M, Ebeling H, Moilanen I, et al. Clinical high-risk state does not predict later psychosis in a delinquent adolescent population. *Early Interv Psychiatry*. 2014;8(1):87–90.
24. Benton MK, Schroeder HE. Social skills training with schizophrenics: a meta-analytic evaluation. *J Consult Clin Psychol*. 1990;58(6):741–7.
25. McGlashan TH, Zipursky RB, Perkins D, Addington J, Miller T, Woods SW, et al. Randomized, double-blind trial of olanzapine versus placebo in patients prodromally symptomatic for psychosis. *Am J Psychiatry*. 2006;163(5):790–9.
26. Ruhrmann S, Bechdolf A, Kuhn KU, Wagner M, Schultze-Lutter F, Janssen B, et al. Acute effects of treatment for prodromal symptoms for people putatively in a late initial prodromal state of psychosis. *Br J Psychiatry Suppl*. 2007;51:s88–95.
27. Woods SW, Tully EM, Walsh BC, Hawkins KA, Callahan JL, Cohen SJ, et al. Aripiprazole in the treatment of the psychosis prodrome: an open-label pilot study. *Br J Psychiatry Suppl*. 2007;51:s96–101.
28. Combs DR, Adams SD, Penn DL, Roberts D, Tiegreen J, Stem P. Social cognition and interaction training (SCIT) for inpatients with schizophrenia spectrum disorders: preliminary findings. *Schizophr Res*. 2007;91(1–3):112–6.
29. McGorry PD, Nelson B, Phillips LJ, Yuen HP, Francey SM, Thampi A, et al. Randomized controlled trial of interventions for young people at ultra-high risk of psychosis: twelve-month outcome. *J Clin Psychiatry*. 2013;74(4):349–56.
30. Amminger GP, Schafer MR, Schlogelhofer M, Klier CM, McGorry PD. Longer-term outcome in the prevention of psychotic disorders by the Vienna omega-3 study. *Nat Commun*. 2015;6:7934.
31. Lappin JM, Dazzan P, Morgan K, Morgan C, Chitnis X, Suckling J, et al. Duration of prodromal phase and severity of volumetric abnormalities in first-episode psychosis. *Br J Psychiatry Suppl*. 2007;51:s123–127.
32. Ho BC. MRI brain volume abnormalities in young, nonpsychotic relatives of schizophrenia probands are associated with subsequent prodromal symptoms. *Schizophr Res*. 2007;96(1–3):1–13.
33. Tognin S, Riecher-Rössler A, Meisenzahl EM, Wood SJ, Hutton C, Borgwardt SJ, et al. Reduced parahippocampal cortical thickness in subjects at ultra-high risk for psychosis. *Psychol Med*. 2014;44(3):489–98.
34. Owens SF, Picchioni MM, Ettinger U, McDonald C, Walshe M, Schmechtig A, et al. Prefrontal deviations in function but not volume are putative endophenotypes for schizophrenia. *Brain*. 2012;135(Pt 7):2231–44.
35. Duffy FH, Als H. A stable pattern of EEG spectral coherence distinguishes children with autism from neuro-typical controls – a large case control study. *BMC Med*. 2012;10(1):64.
36. Hughes JR, John ER. Conventional and quantitative electroencephalography in psychiatry. *J Neuropsychiatry Clin Neurosci*. 1999;11(2):190–208.
37. van Drongelen W. Signal processing for neuroscientists: an introduction to the analysis of physiological signals, vol. 5. Oxford: Elsevier; 2011.
38. Press WH, Teukolsky SA, Vetterling WT, Flannery BP. *Numerical Recipes in C: The Art of Scientific Computing*. 2nd ed. Cambridge: Cambridge University Press; 1995.
39. Srinivasan V, Eswaran C, Sriaram N. Approximate entropy-based epileptic EEG detection using artificial neural networks. *IEEE Trans Inf Technol Biomed*. 2007;11(3):288–95.
40. Morigisa JM, Duffy FH, Wyatt RJ. Topographic analysis of computer processed electroencephalography in schizophrenia. In: Usdin E, Hanin I, editors. *Biological markers in neurology and psychiatry*. New York: Pergamon Press; 1982. p. 495–504.
41. Morstyn R, Duffy FH, McCarley RW. Altered topography of EEG spectral content in schizophrenia. *Electroencephalogr Clin Neurophysiol*. 1983;65:263–71.
42. Karson CN, Coppola R, Morigisa JM, Weinberger DR. Computed electroencephalographic activity mapping in Schizophrenia: the resting state reconsidered. *Arch Gen Psychiatry*. 1987;44(6):514–7.
43. Stevens JR. Disturbances of ocular movements and blinking in schizophrenia. *J Neurol Neurosurg Psychiatry*. 1978;41(11):1024–30.
44. Henshall KR, Sergejew AA, Rance G, McKay CM, Copolov DL. Interhemispheric EEG coherence is reduced in auditory cortical regions in schizophrenia patients with auditory hallucinations. *Int J Psychophysiol*. 2013;89(1):63–71.
45. Kam JW, Bolbecker AR, O'Donnell BF, Hetrick WP, Brenner CA. Resting state EEG power and coherence abnormalities in bipolar disorder and schizophrenia. *J Psychiatr Res*. 2013;47(12):1893–901.
46. Mann K, Maier W, Franke P, Roschke J, Gansicke M. Intra- and interhemispheric electroencephalogram coherence in siblings discordant for schizophrenia and healthy volunteers. *Biol Psychiatry*. 1997;42(8):655–63.
47. Nagase Y, Okubo Y, Matsuura M, Kojima T, Toru M. EEG coherence in unmedicated schizophrenic patients: topographical study of predominantly never medicated cases. *Biol Psychiatry*. 1992;32:1028–34.
48. Pachou E, Vourkas M, Simos P, Smit D, Stam CJ, Tsirka V, et al. Working memory in schizophrenia: an EEG study using power spectrum and coherence analysis to estimate cortical activation and network behavior. *Brain Topogr*. 2008;21(2):128–37.
49. Wada Y, Nanbu Y, Jiang ZY, Koshino Y, Hashimoto T. Interhemispheric EEG coherence in never-medicated patients with paranoid schizophrenia: analysis at rest and during photic stimulation. *Clin EEG*. 1998;29(4):170–6.
50. Wada Y, Nanbu Y, Kikuchi M, Koshino Y, Hashimoto T. Aberrant functional organization in schizophrenia: analysis of EEG coherence during rest and photic stimulation in drug-naive patients. *Neuropsychobiology*. 1998;38(2):63–9.
51. Andreou C, Nolte G, Leicht G, Polomac N, Hanganu-Opatz IL, Lambert M, et al. Increased resting-state gamma-band connectivity in first-episode schizophrenia. *Schizophr Bull*. 2015;41(4):930–9.
52. Bandyopadhyaya D, Nizamie SH, Pradhan N, Bandyopadhyaya A. Spontaneous gamma coherence as a possible trait marker of schizophrenia – an explorative study. *Asian J Psychiatr*. 2011;4(3):172–7.
53. Chen CM, Stanford AD, Mao X, Abi-Dargham A, Shungu DC, Lisnby SH, et al. GABA level, gamma oscillation, and working memory performance in schizophrenia. *Neuroimage Clin*. 2014;4:531–9.
54. Diez A, Suazo V, Casado P, Martin-Loeches M, Molina V. Gamma power and cognition in patients with schizophrenia and their first-degree relatives. *Neuropsychobiology*. 2014;69(2):12012–8.
55. Diez A, Suazo V, Casado P, Martin-Loeches M, Perea MV, Molina V. Frontal gamma noise power and cognitive domains in schizophrenia. *Psychiatry Res*. 2014;221(1):104–13.
56. Herrmann CS, Demiralp T. Human EEG gamma oscillations in neuropsychiatric disorders. *Clin Neurophysiol*. 2005;116(12):2719–33.
57. Khan S, Gramfort A, Shetty NR, Kitzbichler MG, Ganesan S, Moran JM, et al. Local and long-range functional connectivity is reduced in concert in autism spectrum disorders. *Proc Natl Acad Sci U S A*. 2013;110(8):3107–12.
58. McNally JM, McCarley RW, Brown RE. Impaired GABAergic neurotransmission in schizophrenia underlies impairments in cortical gamma band oscillations. *Curr Psychiatry Rep*. 2013;15(3):346.
59. Roach BJ, Ford JM, Hoffman RE, Mathalon DH. Converging evidence for gamma synchrony deficits in schizophrenia. *Suppl Clin Neurophysiol*. 2013;62:163–80.
60. Roach BJ, Mathalon DH. Event-related EEG time-frequency analysis: an overview of measures and an analysis of early gamma band phase locking in schizophrenia. *Schizophr Bull*. 2008;34(5):907–26.
61. Whitham EM, Pope KJ, Fitzgibbon SP, Lewis T, Clark CR, Loveless S, et al. Scalp electrical recording during paralysis: quantitative evidence that EEG frequencies above 20 Hz are contaminated by EMG. *Clin Neurophysiol*. 2007;118(8):1877–88.
62. Whitham EM, Lewis T, Pope KJ, Fitzgibbon SP, Clark CR, Loveless S, et al. Thinking activates EMG in scalp electrical recordings. *Clin Neurophysiol*. 2008;119(5):1166–75.

63. Yuval-Greenberg S, Tomer O, Keren AS, Nelken I, Deouell LY. Transient induced gamma-band response in EEG as a manifestation of miniature saccades. *Neuron*. 2008;58(3):429–41.
64. Yuval-Greenberg S, Deouell LY. The broadband-transient induced gamma-band response in scalp EEG reflects the execution of saccades. *Brain Topogr*. 2009;22(1):3–6.
65. Melloni L, Schwiedrzik CM, Wibral M, Rodriguez E, Singer W. Response to: Yuval-Greenberg et al., 'Transient induced gamma-band response in EEG as a manifestation of miniature saccades.' *Neuron* 58, 429–441. *Neuron*. 2009;62(1):8–10. Author reply 10–12.
66. Yuval-Greenberg S, Deouell LY. Scalp-recorded induced gamma-band responses to auditory stimulation and its correlations with saccadic muscle-activity. *Brain Topogr*. 2011;24(1):30–9.
67. Oertel-Knochel V, Bittner RA, Knochel C, Prvulovic D, Hampel H. Discovery and development of integrative biological markers for schizophrenia. *Prog Neurobiol*. 2011;95(4):686–702.
68. Duffy FH, Eksioglu YZ, Rotenberg A, Madsen JR, Shankardass A, Als H. The frequency modulated auditory evoked response (FMAER), a technical advance for study of childhood language disorders: cortical source localization and selected case studies. *BMC Neurol*. 2013;13(1):1–22.
69. Duffy FH, Shankardass A, McAnulty GB, Eksioglu YZ, Coulter D, Rotenberg A, et al. Corticosteroid therapy in regressive autism: a retrospective study of effects on the Frequency Modulated Auditory Evoked Response (FMAER), language, and behavior. *BMC Neurol*. 2014;14:70.
70. Fulham WR, Michie PT, Ward PB, Rasser PE, Todd J, Johnston PJ, et al. Mismatch negativity in recent-onset and chronic schizophrenia: a current source density analysis. *PLoS One*. 2014;9(6):e100221.
71. Oertel-Knochel V, Knochel C, Matura S, Stablein M, Prvulovic D, Maurer K, et al. Association between symptoms of psychosis and reduced functional connectivity of auditory cortex. *Schizophr Res*. 2014;160(1–3):35–42.
72. Oertel-Knochel V, Knochel C, Matura S, Prvulovic D, Linden DE, van de Ven V. Reduced functional connectivity and asymmetry of the planum temporale in patients with schizophrenia and first-degree relatives. *Schizophr Res*. 2013;147(2–3):331–8.
73. Bartels PH. Numerical evaluation of cytologic data. IX. Search for data structure by principal components transformation. *Anal Quant Cytol*. 1981;3(3):167–77.
74. Duffy FH, Jones K, Bartels P, McAnulty G, Albert M. Unrestricted principal components analysis of brain electrical activity: Issues of data dimensionality, artifact, and utility. *Brain Topogr*. 1992;4(4):291–307.
75. Duffy FH. Issues facing the clinical use of brain electrical activity. In: Pfurtscheller G, Lopes Da Silva F, editors. *Functional Brain Imaging*. Stuttgart: Hans Huber Publishers; 1988. p. 149–60.
76. Diagnostic Interview: Kiddie-Sads-Present and Lifetime. Version (K-SADS-PL). <http://www.psychiatry.pitt.edu/sites/default/files/Documents/assessments/ksads-pl.pdf>.
77. Lu Z, Heeramun-Aubeeluck A. Cognitive markers in schizophrenia prodrome: a review. *ASEAN J Psychiatry*. 2012;13:1–21.
78. Miller TJ, McGlashan TH, Woods SW, Stein K, Driesen N, Corcoran CM, et al. Symptom assessment in schizophrenic prodromal states. *Psychiatr Q*. 1999;70(4):273–87.
79. McGlashan TH, Miller TJ, Woods SW, Hoffman RE, Davidson L. A scale for the assessment of prodromal symptoms and states. In: Miller TJ, Mednick SA, McGlashan TH, Libiger J, Johannessen JO, editors. *Early Intervention in Psychotic Disorders*. Dordrecht: Kluwer Academic Publishing; 2001. p. 135–50.
80. McGlashan TH, Walsh BC, Woods DL. *Structured Interview for Psychosis – Risk Syndromes, Version 5.0*. New Haven: Prime Research Clinic; Yale School of Medicine; 2010.
81. Bruininks R, Woodcock R, Weatherman R. *Scales of independent behavior – revised*. Rolling Meadows: Riverside Publishing; 1997.
82. Green GGR, Kay RH, Rees A. Responses evoked by frequency-modulated sounds recorded from the human scalp. *J Physiol*. 1979;296:21–22P.
83. Green GGR, Rees A, Stefanatos GA. A method for recording evoked responses to frequency modulated sounds in man. *J Physiol*. 1980;307:10p.
84. Stefanatos GA. Speech perceived through a damaged temporal window: lessons from word deafness and aphasia. *Semin Speech Lang*. 2008;29(3):239–52.
85. Stefanatos GA, Foley C, Grover W, Doherty B. Steady-state auditory evoked responses to pulsed frequency modulations in children. *Electroencephalogr Clin Neurophysiol*. 1997;104:31–42.
86. Stefanatos GA, Green GGR, Ratcliff GG. Neurophysiological evidence of auditory channel anomalies in developmental dysphasia. *Arch Neurol*. 1989;46(8):871–5.
87. Berg P, Scherg M. Dipole modeling of eye activity and its application to the removal of eye artifacts from EEG and MEG. *Clin Phys Physiol Meas*. 1991;12(Suppl A):49–54.
88. Berg P, Scherg M. A multiple source approach to the correction of eye artifacts. *Electroencephalogr Clin Neurophysiol*. 1994;90:229–41.
89. Lins OG, Picton TW, Berg P, Scherg M. Ocular artefacts in recording EEGs and event related potentials II: Source dipoles and source components. *Brain Topogr*. 1993;6:65–78.
90. Srinivasan R, Winter WR, Ding J, Nunez PL. EEG and MEG coherence: measures of functional connectivity at distinct spatial scales of neocortical dynamics. *J Neurosci Methods*. 2007;166(1):41–52.
91. Semlitsch HV, Anderer P, Schuster P, Presslich O. A solution for reliable and valid reduction of ocular artifacts, applied to the P300 ERP. *Psychophysiology*. 1986;23(6):695–703.
92. Dixon WJ. *BMDP Statistical Software Manual: To accompany BMDP 7.0 software release*. Berkeley: University of California Press; 1992.
93. Bartels PH. Numerical evaluation of cytologic data VIII. Computation of the principal components. *Anal Quant Cytol*. 1981;3(2):83–90.
94. Martinez LM, Martinez AR, Solka JL. *Exploratory Data Analysis with MATLAB*. Second Edition ed. London: Chapman and Hall/CRC; 2011.
95. Han J, Kamber M, Pei J. *Data Mining, Concepts and Techniques*. 3rd ed. Boston: Morgan Kaufmann; 2012.
96. Cooley WW, Lohnes PR. *Multivariate Data Analysis*. New York: Wiley; 1971.
97. Duffy FH, Burchfiel JL, Lombroso CT. Brain electrical activity mapping (BEAM): a method for extending the clinical utility of EEG and evoked potential data. *Ann Neurol*. 1979;5:309–21.
98. Duffy FH, Bartels PH, Burchfiel JL. Significance probability mapping: an aid in the topographic analysis of brain electrical activity. *Electroencephalogr Clin Neurophysiol*. 1981;51:455–62.
99. Duffy FH, Jones KH, McAnulty GB, Albert MS. Spectral coherence in normal adults: unrestricted principal components analysis – relation of factors to age, gender, and neuropsychologic data. *Clin EEG*. 1995;26(1):30–46.
100. Duffy FH, Als H, McAnulty GB. Infant EEG spectral coherence data during quiet sleep: unrestricted principal components analysis – relation of factors to gestational age, medical risk, and neurobehavioral status. *Clin EEG*. 2003;34(2):54–69.
101. Duffy FH, McAnulty GM, McCreary MC, Cuchural GJ, Komaroff AL. EEG spectral coherence data distinguish chronic fatigue syndrome patients from healthy controls and depressed patients – a case control study. *BMC Neurol*. 2011;11:82.
102. Duffy F, Shankardass A, McAnulty G, Als H. The relationship of Asperger's syndrome to autism: a preliminary EEG coherence study. *BMC Med*. 2013;11:175.
103. Bartels PH. Numerical evaluation of cytologic data IV. Discrimination and classification. *Anal Quant Cytol*. 1980;2(1):19–24.
104. Marascuilo LA, Levin JR. *Multivariate Statistics in the Social Sciences: A Researchers Guide*. Monterey: Brooks/Cole Publishing Co.; 1983.
105. Lachenbruch PA, Mickey RM. Estimation of error rates in discriminant analysis. *Technometrics*. 1968;10:1–11.
106. Lachenbruch PA. *Discriminant Analysis*. New York: Hafner Press; 1975.
107. Chernick MR. *Bootstrap Methods: A Guide for Practitioners and Researchers*. 2nd ed. Hoboken: Wiley; 2008.
108. Dixon WJ. *BMDP Statistical Software (revised edition)*. Berkeley: University of California Press; 1985.
109. Foley DH. Consideration of sample and feature size. *IEEE Trans Inform Theory*. 1972;18(5):618–26.
110. Bartels PH. Numerical evaluation of cytologic data III. Selection of features for discrimination. *Anal Quant Cytol*. 1979;1:153–9.
111. Arnold SE. The medial temporal lobe in schizophrenia. *J Neuropsychiatry Clin Neurosci*. 1997;9(3):460–70.
112. Cullen AE, De Brito SA, Gregory SL, Murray RM, Williams SC, Hodgins S, et al. Temporal lobe volume abnormalities precede the prodrome: a study of children presenting antecedents of schizophrenia. *Schizophr Bull*. 2013;39(6):1318–27.
113. Lawrie SM, Whalley HC, Abukmeil SS, Kestelman JN, Miller P, Best JJ, et al. Temporal lobe volume changes in people at high risk of schizophrenia with psychotic symptoms. *Br J Psychiatry*. 2002;181:138–43.
114. Mathew I, Gardin TM, Tandon N, Eack S, Francis AN, Seidman LJ, et al. Medial temporal lobe structures and hippocampal subfields in psychotic

- disorders: findings from the Bipolar-Schizophrenia Network on Intermediate Phenotypes (B-SNIP) study. *JAMA Psychiatry*. 2014;71(7):769–77.
115. Roth WT, Pfefferbaum A. Abnormalities of the left temporal lobe in schizophrenia. *N Engl J Med*. 1992;327(23):1689–90.
 116. Shenton ME, Kikinis R, Jolesz FA, Pollak SD, LeMay M, Wible CG, et al. Abnormalities of the left temporal lobe and thought disorder in schizophrenia. A quantitative magnetic resonance imaging study. *NEJM*. 1992;327(9):604–12.
 117. Smiley JF, Rosoklija G, Mancevski B, Pergolizzi D, Figarsky K, Bleiwas C, et al. Hemispheric comparisons of neuron density in the planum temporale of schizophrenia and nonpsychiatric brains. *Psychiatry Res*. 2011;192(1):1–11.
 118. Suddath RL, Casanova MF, Goldberg TE, Daniel DG, Kelsoe Jr JR, Weinberger DR. Temporal lobe pathology in schizophrenia: a quantitative magnetic resonance imaging study. *Am J Psychiatry*. 1989;146(4):464–72.
 119. Sundram F, Cannon M, Doherty CP, Barker GJ, Fitzsimons M, Delanty N, et al. Neuroanatomical correlates of psychosis in temporal lobe epilepsy: voxel-based morphometry study. *Br J Psychiatry*. 2010;197(6):482–92.
 120. Covington MA, He C, Brown C, Naci L, McClain JT, Fjordbak BS, et al. Schizophrenia and the structure of language: the linguist's view. *Schizophr Res*. 2005;77(1):85–98.
 121. Thermenos HW, Whitfield-Gabrieli S, Seidman LJ, Kuperberg G, Juelich RJ, Divatia S, et al. Altered language network activity in young people at familial high-risk for schizophrenia. *Schizophr Res*. 2013;151(1–3):229–37.
 122. Mou X, Bai F, Xie C, Shi J, Yao Z, Hao G, et al. Voice recognition and altered connectivity in schizophrenic patients with auditory hallucinations. *Prog Neuropsychopharmacol Biol Psychiatry*. 2013;44:265–70.
 123. Lisman J. Excitation, inhibition, local oscillations, or large-scale loops: what causes the symptoms of schizophrenia? *Curr Opin Neurobiol*. 2012;22:537–44.
 124. Lisman JE, Pi HJ, Zhang Y, Otmakhova NA. A thalamo-hippocampal-ventral tegmental area Loop may produce the positive feedback that underlies the psychotic break in schizophrenia. *Biol Psychiatry*. 2010;68:17–24.
 125. Zhang Y, Llinas RR, Lisman JE. Inhibition of NMDARs in the nucleus reticularis of the thalamus produces delta frequency bursting. *Front Neural Circuits*. 2009;3:1–9.

**Submit your next manuscript to BioMed Central
and take full advantage of:**

- Convenient online submission
- Thorough peer review
- No space constraints or color figure charges
- Immediate publication on acceptance
- Inclusion in PubMed, CAS, Scopus and Google Scholar
- Research which is freely available for redistribution

Submit your manuscript at
www.biomedcentral.com/submit

